Pol. J. Environ. Stud. Vol. 34, No. 5 (2025), 5203-5214
DOI: *10.15244/pjoes/191020* ONLINE PUBLICATION DATE: 2025-03-10

Original Research

Study on the Adsorption Characteristics of Pb(II) in Water by Apatite-Modified Biochar

Haihua Li*, Zihan Chen, Lu Yu, Zihan Chen, Baozeng Xiao, Kaili Jin

School of Environmental and Municipal Engineering, North China University of Water Resources and Electric Power, Zhengzhou, China

Received: 5 April 2024
Accepted: 9 July 2024

Abstract

In this study, biochar was prepared using sesame straw and treated with slightly soluble phosphate. The removal effect, adsorption mechanism, and influencing factors of biochar on Pb(II) in water were determined using batch adsorption experiments. Chlorapatite-modified biochar (BC-Cl) and hydroxyapatite-modified biochar (HBC) were prepared by co-impregnating the original biochar (BC) with hydroxyapatite and BC. The results showed that BC-Cl exhibited the best removal effect on heavy metal Pb(II) at pH = 5 and a dosage of 600 $mg \cdot L^{-1}$. The adsorption of Pb(II) by BC-Cl was in line with the pseudo-second-order kinetic equation and the Langmuir isothermal adsorption model, indicating that the adsorption process was dominated by chemical adsorption and monolayer adsorption. Additionally, phosphorus was essential in the adsorption of Pb(II) by the modified biochar. The main reason for the high removal rate of Pb(II) by BC-Cl is that PO_4^{3-} produced via chloroapatite dissolution can precipitate with Pb(II) and then generate insoluble phosphate precipitation in water. In summary, the inorganic material apatite-modified sesame straw biochar has excellent application potential as it has a high removal rate and excellent adsorption performance for Pb(II) in water.

Keywords: Sesame straw, chloroapatite, modified biochar, lead wastewater, adsorption mechanism

Introduction

Copper, nickel, mercury, arsenic, chromium, cadmium, zinc, and lead are among the common toxic heavy metals stipulated by the World Health Organization (WHO) [1]. Among them, lead is widely used in industry because of its low price and abundant production, but it will produce a lot of wastewater and waste residue containing Pb(II) in the production process. Wastewater containing Pb(II) discharged into the natural environment without adequate treatment will pose a serious threat to ecological security [2, 3]. In particular, Pb(II) in natural water bodies has high mobility, which is easy to accumulate in the human body through the biological chain, causing a serious impact on human health [4-6]. Therefore, it is particularly important to find an efficient, low-cost, and convenient method to remove Pb(II) from lead-containing wastewater. Among the various methods, adsorption is considered to be a very feasible method due to its environmental friendliness, versatility, and simplicity [7, 8].

Biochar produced by pyrolysis of waste biomass in the process of agricultural production under

*e-mail: lihaihua918@163.com

the conditions of high temperature and limited oxygen has been widely studied because of its advantages of a simple preparation process, low price, and wide source [9-11]. The results show that sesame straw is rich in cellulose, minerals, and organic matter and is a high-quality raw material for preparing biochar [12, 13]. Therefore, using sesame straw as a raw material to prepare raw biochar (BC) for wastewater treatment can not only improve its value, but also reduce the input of its treatment and disposal [14]. However, the adsorption capacity of pure BC to Pb(II) is limited by its porosity and functional groups [15]. In order to improve the adsorption properties of BC, many modification methods have been extensively studied. These methods include co-pyrolysis modification, acid-base modification, co-impregnation, and so on [16-18]. Among the existing modification methods, there is plenty of research on co-pyrolysis of BC with other adsorbents, but few studies on co-impregnation of BC [19, 20].

Apatite includes chlorapatite ($Ca_5(PO_4)_3Cl$) and hydroxyapatite ($Ca_5(PO_4)_3OH$), which is non-toxic, low-cost, has and low water solubility, so it is considered to be an environmentally friendly adsorbent [21]. A large number of studies have shown that apatite has an efficient removal capacity of heavy metals through ion exchange, surface complex formation, and solution-precipitation mechanisms [22]. However, the high surface area of apatite makes it easy to self-aggregate, which greatly reduces its adsorption performance [23]. Considering the characteristics of apatite and BC, it may be an ideal way to combine them into a new absorbent. Therefore, in this study, chlorapatite and hydroxyapatite were co-impregnated and combined with BC to prepare chlorapatite modified biochar (BC-Cl) and hydroxyapatite modified biochar (HBC), and the adsorption effects of BC-Cl and HBC on Pb(II) were compared and analyzed.

In this paper, apatite was used to modify BC by co-impregnation, and the material properties of BC, HBC, and BC-Cl were characterized and analyzed by elemental analysis, X-ray photoelectron spectroscopy (XPS), X-ray diffractometer (XRD), and Fourier transform infrared spectroscopy (FT-IR). Adsorption experiments were designed to investigate the removal capacity and potential adsorption mechanism of Pb(II) from polluted wastewater by BC, HBC, and BC-Cl. This work provides a basis for the application of BC-Cl in high-efficiency adsorption of Pb(II) in water and provides a new way for the resource utilization of sesame straw.

Material and Methods

Biochar Preparation

Preparation of BC: The BC was prepared using limited oxygen pyrolysis in a muffle furnace with a temperature controller. During pyrolysis, the temperature was raised to 550ºC at a heating rate of 10ºC min^{-1} and maintained for 2 h. After the crucible was reduced to room temperature, it was taken out, washed with deionized water 2–3 times to remove impurities, and dried to a constant weight at 55ºC. The obtained sample was marked as BC (biochar) and was ground and sealed using a 20-mesh sieve.

Preparation of BC-Cl: After pyrolysis, 2, 3, and 5 g of biochar were weighed in a beaker, and 50 ml of a 0.334 mol L^{-1} $CaCl_2$ solution was added to it. The mixture was stirred vigorously for 30 min with a magnetic stirrer, and 50 ml of a 0.2 mol L^{-1} $(NH_4)2HPO_4$ solution was added dropwise to the mixture at a rate of 6-7 drops per minute (both of which underwent a co-precipitation reaction to form chloroapatite) and stirred for 2 h. After stirring, the mixture was allowed to stand for 24 h [24, 25], after which it was washed 2-3 times with anhydrous ethanol, washed 3 times with deionized water, dried to a constant weight at 55ºC, ground, and sieved through a 20-mesh sieve. After the preparation, the biochar composites were labeled as BC-Cl1 (2 g), BC-Cl2 (3 g), and BC-Cl3 (5 g).

Preparation of HBC: After pyrolysis, 5 g of biochar was weighed in a beaker, and 50 ml of $CaCl_2$ solution (0.334 mol L^{-1}) was added to it. The solution was stirred vigorously for 30 min with a magnetic stirrer, and 50 ml of a 0.2 mol L^{-1} $(NH_4)2HPO_4$ solution was added to it at a rate of 6-7 drops per minute and tuned with ammonia to maintain a pH = 10 (the two co-precipitated to form hydroxyapatite). The mixture was stirred for 2 h after dripping and maintained for 24 h after stirring. It was washed 2-3 times with anhydrous ethanol, washed 3 times with deionized water, dried to a constant weight at 55ºC, ground, and sieved through a 20-mesh sieve for storage. After the preparation, the biochar composite material was labeled as HBC.

Characterization of Biochar Materials

The pH values of the BC and BC-Cl were determined using a (PHS-3C) pH meter after the water and biochar were combined at a mass ratio of 20:1. The physicochemical properties of the three biochar types were analyzed; the elemental composition of the material was analyzed using XPS, and C and O were subjected to deconvolution integral peak treatment. FTIR was used to characterize the samples, and the type and number of functional groups were determined by qualitatively analyzing the wavelength changes; the mineral composition and crystallization of the biochar samples were measured using XRD.

Experimental Method

Firstly, 0.3997±0.0001 g of $Pb(NO_3)_2$ (analytical purity) was added into a 1 L beaker, dissolved with deionized water and a little concentrated nitric acid, and continuously stirred using a magnetic stirrer. During this period, sodium hydroxide and dilute nitric acid

were used to regulate the pH, and a 1 L volumetric flask was used to set the volume. As a result, a Pb(II) solution with a mass concentration of 250 mg·L^{-1} was prepared. Three parallel samples were set for each adsorption experiment below.

Comparison and Selection of Biochar from Different Materials

A 100 ml conical flask was filled with 30 mg of three different kinds of biochar (BC, BC-Cl, and HBC), and 50 ml of a 250 mg·L^{-1} Pb(II) solution with a pH of 5 was added to the conical flask. After gently shaking and mixing, the flask was placed in a thermostatic oscillator to oscillate for 24 h. The temperature was maintained at 25ºC, and the oscillation rate was 120 r·min^{-1}. After the oscillation, the solution was filtered with a 0.45 μm filter membrane, and the filtered solution was refrigerated in a refrigerator for measurement. The material with the best adsorption effect was selected for subsequent experiments based on the adsorption degree.

The Effect of Different pH Levels on the Adsorption of Pb(II)

A conical flask weighing 30 mg of BC-Cl was filled with 50 ml of a 250 mg·L^{-1} Pb(II) solution, and the pH of the system was adjusted to 3.0, 4.0, 5.0, 6.0, 7.0, and 8.0. The remaining operations were consistent with the abovementioned operation. The effect of different pHs on Pb(II) adsorption was studied using the adsorption capacity.

Effect of Adsorbent Dosage on Adsorption of Pb(II)

A conical flask was weighed with 10 mg, 20 mg, 30 mg, 40 mg, 50 mg, 80 mg, and 100 mg of BC-Cl, and 50 ml of a 250 mg·L^{-1} Pb(II) solution with an adjusted pH of 5.0 was added to the conical flask. The other operations were consistent with the abovementioned operation. The effect of different adsorbent dosages on Pb(II) adsorption was studied using adsorption capacity.

Kinetic Adsorption Experiment

First, 30 mg of BC-Cl was weighed in a conical flask, and 50 ml of a 250 mg·L^{-1} Pb(II) solution with an adjusted pH of 5.0 was added. After shaking gently, it was placed in a thermostatic oscillator for reaction for 15 min, 30 min, 45 min, 1 h, 1.5 h, 2 h, 4 h, 6 h, 8 h, 12 h, 18 h, 24 h, and 36 h; the rest of the operation was consistent with the abovementioned operation.

Isothermal Adsorption Experiment

First, 30 mg of BC-Cl was weighed in a conical flask, and 50 ml of a 250 mg·L^{-1} Pb(II) solution with an adjusted pH of 5.0 was added. After gently oscillating, the solution was placed in a constant temperature oscillator for 24 h, and the temperature was maintained at 25ºC, 35ºC, and 45ºC. The oscillation rate was set at 120 r·min^{-1}. After the oscillation, the solution was filtered with a 0.45 μm filter membrane, and the filtered solution was refrigerated in the refrigerator for measurement.

Data Processing

The removal rate and adsorption amount of the heavy metal by biochar were calculated using the following formulas:

$$R = \frac{C_0 - C}{C_0} \times 100\% \quad (1)$$

$$q_t = \frac{V\ (C_0 - C_t)}{m} \quad (2)$$

Where R is the removal rate of heavy metals in water (%), C0 is the concentration of heavy metal pollutants before adsorption (mg·L^{-1}), C is the concentration of heavy metal pollutants after adsorption (mg·L^{-1}), qt is the adsorption capacity at time t (mg/g), V is the volume of the solution (ml), Ct is the concentration of heavy metal pollutants at time t (mg·L^{-1}), and m is the adsorbent (mass of biochar) (g).

The adsorption kinetic fitting was calculated using formulas (3) (pseudo-first-order kinetic equation), (4) (pseudo-second-order kinetic equation), and (5) (Elovich model) [26].

$$Q_t = Q_e(1\text{-}e^{-k_1 t}) \quad (3)$$

$$Q_t = \frac{k_2 Q_e^2 t}{1+k_2 Q_e t} \quad (4)$$

$$Q_t = \alpha + \beta \ln t, \quad (5)$$

Where Qt is the adsorption capacity of biochar to heavy metals at time t (mg/g), Q_e is the adsorption capacity of biochar to heavy metals at adsorption equilibrium (mg/g), k_1 is the adsorption rate constant (min^{-1}), k_2 is the adsorption rate constant (min^{-1}), α is the adsorption rate constant, and β is the proportional coefficient.

The adsorption isotherm fitting was calculated using formulas (6) (Langmuir isotherm model) and (7) (Freundlich isotherm model) [27].

$$Q_e = \frac{Q_m K C_e}{1+KC_e} \quad (6)$$

$$Q_e = K_f C_e^n, \quad (7)$$

Where Qe is the adsorption capacity of biochar to heavy metals at adsorption equilibrium (mg/g),

Q_m is the theoretical maximum adsorption capacity of biochar to heavy metals (mg/g), K is the adsorption equilibrium constant (L/mg), Ce is the concentration of heavy metals in the equilibrium solution ($mg \cdot L^{-1}$), K_f is the equilibrium constant (L/g), and n is a heterogeneity index, which represents the binding strength between the adsorbent and the heavy metal.

Results and Discussion

Characterization

Elemental Analysis of Biochar

As shown in Table 1, the original biochar samples were alkaline, and the pH values of the BC-Cl and HBC were lower than those of BC after impregnation with phosphate chlorapatite and hydroxyapatite. Additionally, the H/C and O/C values of BC-Cl were higher than those of BC, and the O/C value of HBC was higher than that of BC, indicating that the addition of chloroapatite and hydroxyapatite can effectively increase the number of hydrogen-containing and oxygen-containing functional groups on the biochar surface.

XPS Results

The full spectra of BC, BC-Cl, and HBC after XPS analysis are shown in Fig. 1 (a), (c), and (e). Compared with BC, the characteristic peak of Ca2p in BC-Cl and HBC was significantly enhanced, while the peak of K2p basically disappeared. The results indicated that there was ion exchange during the preparation of BC-Cl and HBC, and calcium ions successfully replaced potassium ions on the surface of biochar. In addition, new characteristic peaks of BC-Cl and HBC appear at 133.37eV, which is mainly attributed to the generation of P 2*p* peaks. In conclusion, the modification of chlorapatite and hydroxyapatite has a great influence on the elemental composition of the sesame straw biochar surface.

The deconvolution spectra of O1s are shown in Fig. 1 (b), (d), and (f). Using Avantage software, the O1s peaks were fitted into three peaks, representing C–OH (532.5 eV), C = O /P = O (531.5 eV), and C–O /P–O (530.5 eV) [28]. Compared with that of BC, the peak area ratio of C–O /P–O in BC-Cl increased from 23.89% to 38.17%, and the change in C = O /P = O ratio was relatively small owing to the increased PO_4^{3-}content in the biochar after composite modification. The C–OH content in the BC-Cl was 21.88% lower than that in BC; this was mainly due to the substitution of some hydrogen ions in the hydroxyl group with Ca^{2+}, which resulted in a significant decrease in its proportion [29]. Additionally, the peak area of C–O/P–O and C = O/P = O in HBC was higher than in the original biochar, which was similar to that in BC-Cl.

FTIR Results

The FTIR spectra of the three biochars are shown in Fig. 2 (a). Compared with BC, the surface functional groups of modified biochar changed significantly. Fig 2 (a) shows that the peaks near 3439 cm^{-1} and 2926 cm^{-1} are generated by the stretching vibration of hydroxyl functional groups and the asymmetric stretching vibration of $–CH_2$, respectively, and these two peaks appear in the FT-IR images of the modified biochar HBC and BC-Cl. The peaks at 1579 cm^{-1} and 1559 cm^{-1} correspond to the vibration of –COOH. Compared with BC, the intensity of the peaks is enhanced in the spectrum of modified biochar, which may be because the addition of chlorapatite is conducive to the increase of the number of acidic functional groups in biochar. In addition, in the infrared spectrum of BC-Cl, a new characteristic peak appeared at 1035 cm^{-1}, and the peak intensity at 566 cm^{-1} was significantly enhanced. Studies have shown that this is related to the vibration absorption of PO_4^{3-} [30]. Chlorapatite was successfully loaded on the biochar and increased the number of oxygen-containing functional groups (phosphate) on the surface of the biochar. HBC exhibited a strong peak at 1042 cm^{-1} and a distinct peak at 565 cm^{-1}, representing the P–O bond. In contrast to that of BC, the types of functional groups in the HBC did not increase significantly, and only new P–O bonds appeared.

XRD Results

The XRD patterns of the three biochars are shown in Fig. 2 (b). The diagram shows that the peak intensity of the BC-Cl diffraction peak was strong, the peak width was narrow, and the new peak and narrow peak of $Ca_5(PO_4)_3Cl$ appeared in the spectrum, indicating that the pure BC-Cl had good crystallinity. The appearance of the characteristic peak indicates that chloroapatite was successfully loaded on the BC-Cl surface; this can provide more effective adsorption sites for biochar and

Table 1. pH value and element composition of biochar samples.

Sample	pH	C (%)	H (%)	O (%)	N (%)	S (%)	H /C	O /C
BC	10.88	70.55	2.215	12.914	0.99	0.281	0.094	0.184
BC-Cl	6.18	55.24	2.152	12.304	0.87	0.209	0.117	0.255
HBC	8.18	55.49	1.719	13.020	1.10	0.088	0.031	0.235

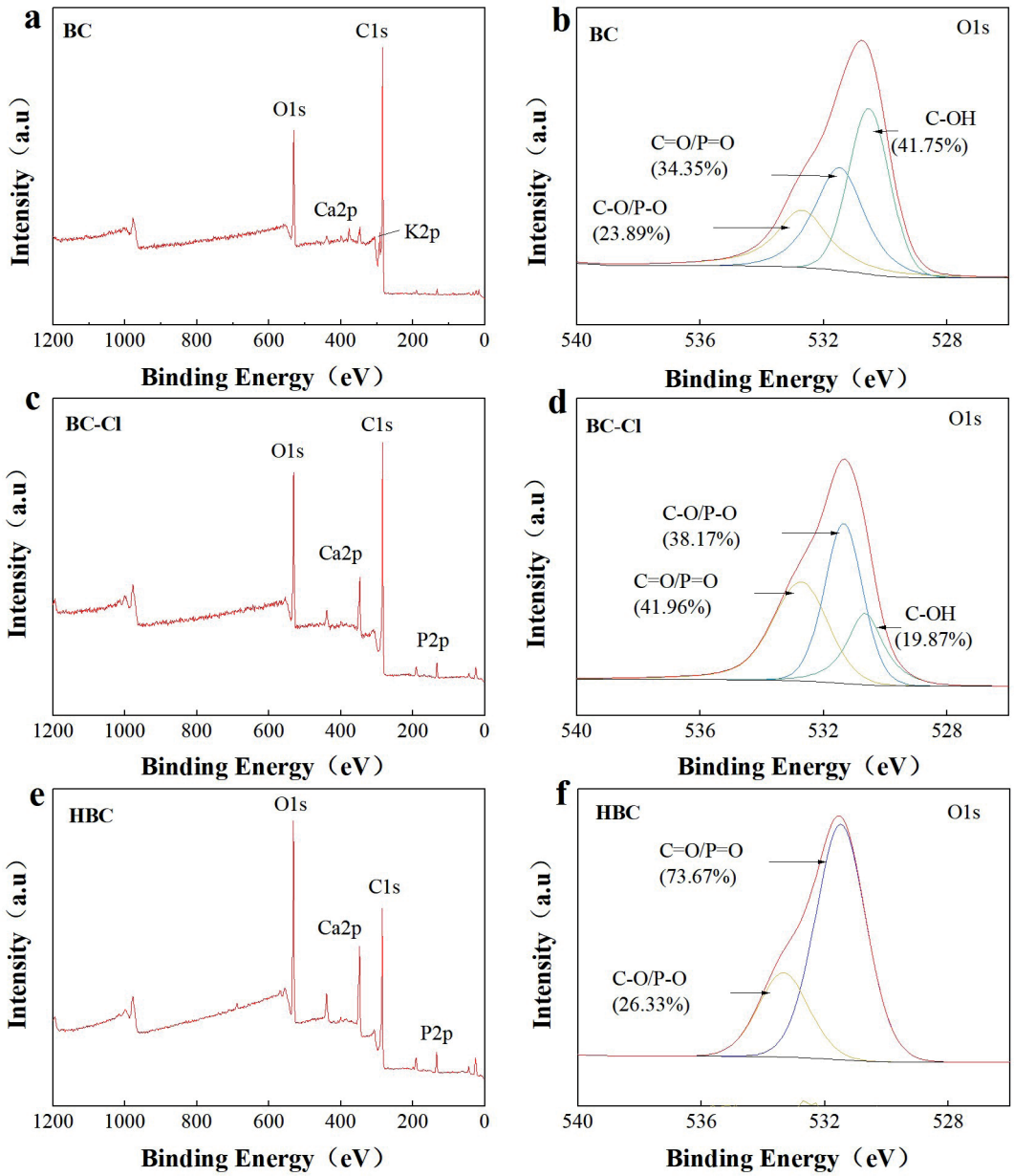

Fig. 1. XPS spectra of BC, BC-Cl, and HBC (a: full spectrum of BC, b: O1s spectra of BC; c: full spectrum of BC-Cl, d: O1s spectra of BC-Cl; e: full spectrum of HBC, f: O1s spectra of HBC).

improve the adsorption effect on heavy metal cations. Similarly, FT-IR spectra also confirmed this result. In addition, the XRD pattern of BC shows that the sesame straw biochar contains calcium carbonate, which may be related to the composition of sesame straw. After hydroxyapatite modification, the characteristic peak of $Ca_5(PO_4)_3OH$ appeared, indicating that the surface of HBC was successfully loaded with hydroxyapatite.

Adsorption Characteristics Study

Batch Adsorption Test

The adsorption results in Fig. 2 (c) showed that the maximum adsorption capacities of BC, BC-Cl, and HBC for Pb(II) were 146.84, 416.16, and 175.53 $mg \cdot g^{-1}$, respectively, and the highest removal rates of Pb(II) were 44.05%, 99.87%, and 47.34%, respectively. After modification, the maximum adsorption capacity of the BC-Cl was 2.83 times that of BC. Combined with the biochar characterization analysis, the sesame straw modified using chlorapatite loading can increase the adsorption capacity of the modified biochar on heavy metal Pb(II) in water, improving its removal rate and significantly increasing the heavy metal adsorption effect of sesame straw biochar. Therefore, BC and BC-Cl3 were finally selected as the materials for the adsorption and removal of heavy metal Pb in aqueous solution in this study.

Effect of pH

The effect of the initial solution pH on the adsorption of Pb(II) in water using modified biochar is shown in Fig. 2 (d), which shows that when the initial pH of the solution continued to increase, the adsorption capacity of BC-Cl3 for lead also increased. Under acidic conditions, the adsorption capacity of biochar for lead increased exponentially as the solution pH gradually increased from 3 to 5, reaching 369.55 mg·g^{-1} and 416.16 mg·g^{-1}. However, when the pH value exceeded 5, the increase in Pb adsorption capacity gradually declined. Some scholars found that at pH = 5.8, Pb(II) forms hydroxide precipitates, making its precipitation pH value higher than at the significant change point [31, 32]. This indicates that the effect of the initial solution pH value on the BC-Cl-induced Pb adsorption is mainly due to the changes in the surface characteristics of biochar, which include the concentration of H^+, the charge degree, and the type of oxygen-containing functional groups.

The Optimum Dosage of BC-Cl

As shown in Fig. 2 (e), as the adsorbent dosage increased, the BC-Cl3-induced removal rate of lead increased rapidly and gradually balanced (i.e., when the adsorbent dosage was 600 mg·L^{-1}, the removal rate was 99.87%). However, in the BC-Cl-induced Pb adsorption process, the unit adsorption capacity gradually decreased; this was mainly due to the increase in adsorbent dosage and the overlap of some adsorption sites in the biochar, which restricted its full utilization [33]. Therefore, considering the removal rate and cost, the optimal dosage of BC-Cl3 for Pb was 600 mg·L^{-1}.

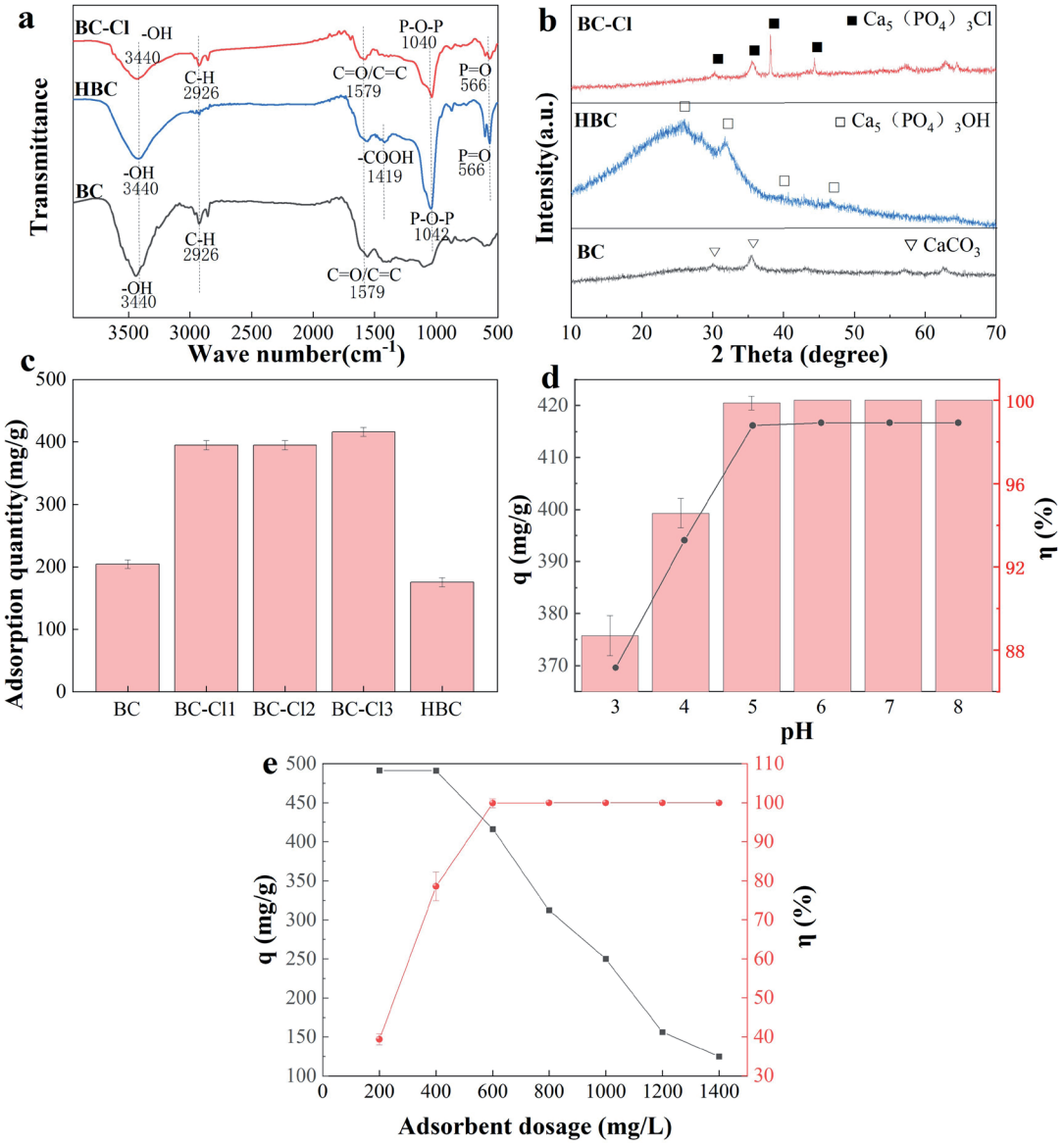

Fig. 2. FT-IR images (a), XRD patterns (b) of BC, BC-Cl, and HBC, comparison of Pb (II) adsorption effects (c), the effect of pH value on Pb (II) adsorption by BC-Cl (d), the effect of BC-Cl dosage on Pb (II) adsorption €.

Adsorption Dynamics

The adsorption kinetics fitting curve of Pb(II) on BC-Cl is shown in Fig. 3. The fitting curve in Fig. 3 shows that at an adsorption time of about 60 min, the BC-Cl-induced adsorption capacity increased rapidly, and the growth rate of adsorption capacity decreased as the adsorption time increased and then gradually reached an adsorption equilibrium state. The adsorption capacity increased rapidly in the early stage of the kinetic adsorption experiment, primarily due to the large number of active sites on the biochar surface at the initial stage of the experiment and the large concentration difference at the adsorbent–water solid–liquid two-phase interface, resulting in a large mass transfer driving force. When the contaminated solution was just added to the conical flask, the concentration of Pb(II) was high, and the mass transfer driving force was also high, speeding up the adsorption rate. Additionally, there were a large number of active sites on the biochar surface at the initial stage of adsorption; this also contributed to the adsorption of Pb(II). With the extension of the oscillation time, the concentration difference between the solid and liquid phases reduced, and the adsorption sites on the biochar surface reduced and gradually tended to be saturated. The diffusion effect inside the modified biochar particles weakened, the adsorption rate decreased, and the adsorption capacity tended to be saturated [29].

In this study, the quasi-first-order kinetic model, quasi-second-order kinetic model, and Elovich model were used to fit the experimental data, and the fitting parameters are shown in Table 2. The results showed that when compared with the Elovich model and the pseudo-first-order kinetics, the pseudo-second-order kinetics better suited the experimental data, and the correlation coefficients, R^2, were 0.771, 0.915, and 1, indicating that the adsorption process was mainly controlled by chemical adsorption [34, 35]; however, the values of the latter two were similar, indicating that physical and chemical adsorption played a positive role in the BC-Cl3-induced Pb(II) adsorption; this was the result of a combination of various adsorption mechanisms.

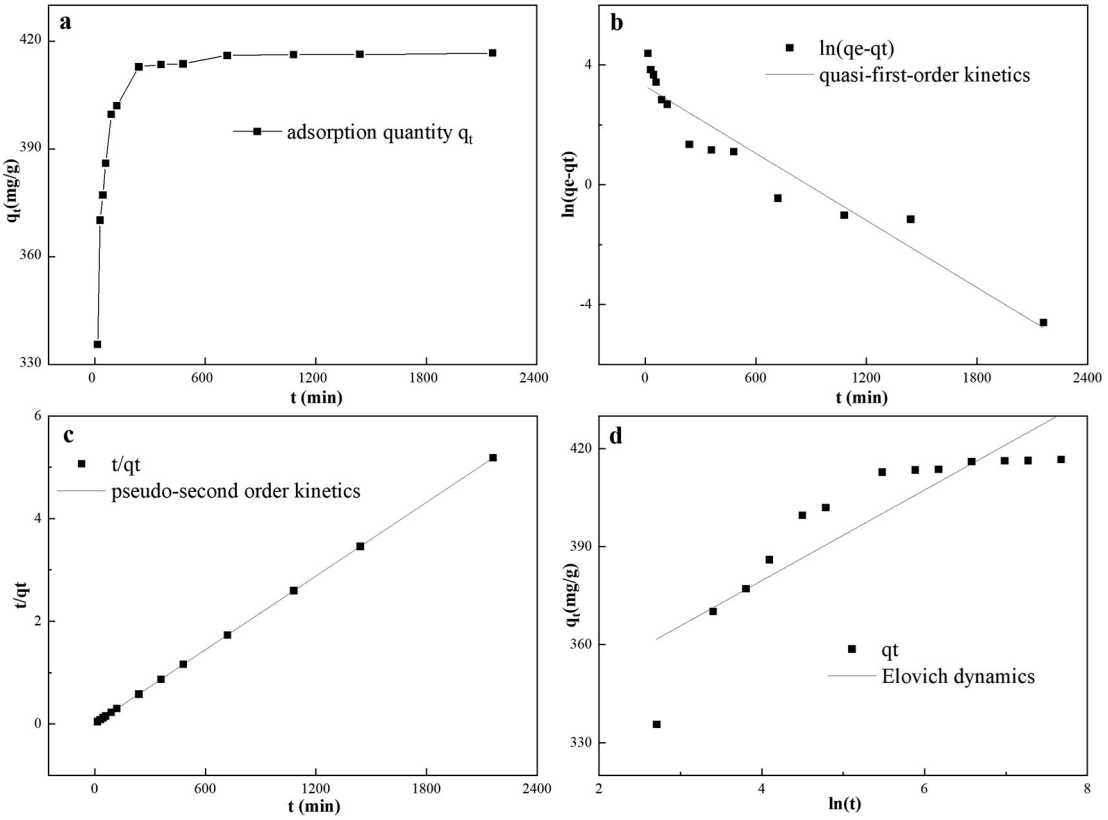

Fig. 3. Adsorption kinetics of Pb(II) on biochar.

Table 2. Kinetic parameters of BC-Cl-induced Pb(II) adsorption.

Specimen	Quasi-first-order kinetics			pseudo-second order kinetics			Elovich		
	Q_e	K_1	R^2	Q_e	K_2	R^2	α	β	R^2
BC-Cl	35.162	0.0037	0.915	418.41	0.0006	1	312.18	11.712	0.771

Adsorption Isotherm

In this study, the Langmuir and Freundlich models were used to fit the experimental data. Fig 4 and Table 3 show that at a temperature of 25ºC, the correlation coefficient, R^2, was relatively large (0.9995) when the BC-Cl3-induced lead adsorption data was fitted with the Langmuir model. The fitting results showed that the theoretical adsorption capacity of BC-Cl3 for lead was up to 529.1 $mg \cdot g^{-1}$, indicating excellent removal ability. At temperatures of 35ºC and 45ºC, the adsorption data could also be well fitted with the Langmuir model, and the correlation coefficients, R^2, were 0.9978 and 0.9997, respectively. This indicates that BC-Cl3 was dominated by monolayer adsorption in the lead adsorption process [36, 37]. The surface of the adsorbent was homogeneous, and there was no interaction between the adsorption sites. This may be because the BC-Cl3 surface contains a large number of lead adsorption sites. When the lead concentration was low, the adsorption process was mainly concentrated on the biochar surface. Additionally, the n value in the Freundlich equation represents the binding strength between biochar and metal cations. The larger the n value, the stronger the adsorption capacity of the biochar [15, 38]. At t = 25ºC, the fitting n value of the BC-Cl3-induced Pb(II) adsorption was 17.61, indicating that BC-Cl had good binding ability to heavy metal Pb and could reduce the risk of dissociation. Additionally, the maximum adsorption capacity calculated using the Langmuir model was close to the experimental value.

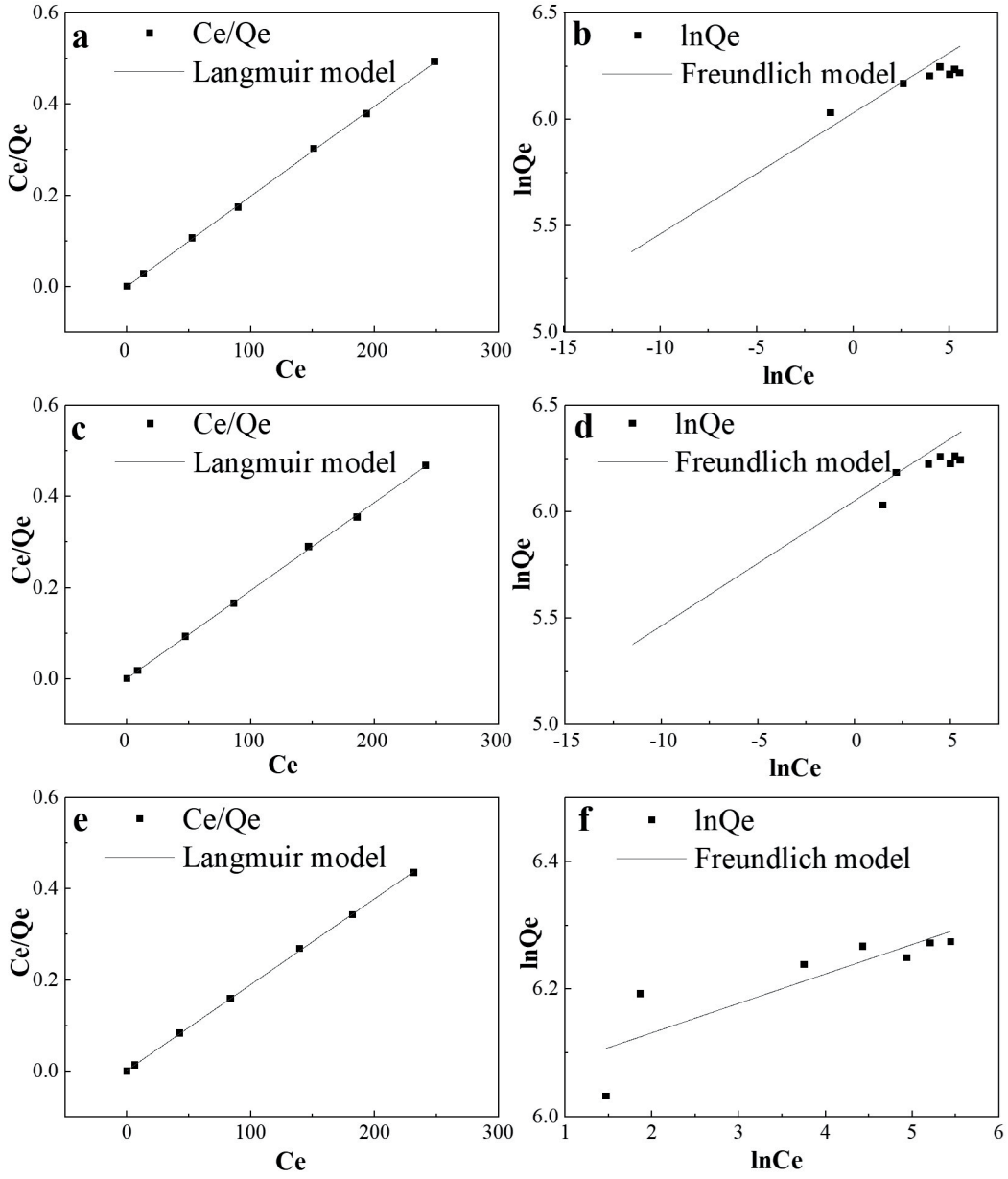

Fig. 4. Fitting curve of biochar to Pb(II) at t = 25ºC, 35ºC, and 45ºC (a,b: 25ºC; c,d: 35ºC; e,f: 45ºC).

Table 3. Isothermal adsorption parameters of Pb(II) on biochar.

Specimen	Temperature	Langmuir			Freundlich		
		K(L/mg)	Q_m(mg/g)	R^2	n	K_f(L/g)	R^2
BC-Cl	25ºC	0.956	505.05	0.9995	17.6056	416.03	0.8229
	35ºC	0.873	518.43	0.9978	17.0357	424.87	0.8323
	45ºC	0.594	529.1	0.9997	21.649	419.56	0.6799

Table 4. Comparison of Pb(II) adsorption performance of BC-Cl and other adsorbents.

Adsorbent	Modifying methods	Equilibrium time/h	Theoretical maximum adsorption capacity /mg.g^{-1}	Reference
Peanut shell biochar	Raw biomass biochar	16	52.99	[39]
Bentonite modified corncob	Bentonite modified	6	109.6	[40]
Magnetic hydroxyapatite /corn straw	Modification of magnetic hydroxyapatite	2	210.85	[41]
Bisporus mushroom bran biochar	Bisporus bran modification	24	266.23	[42]
Calcium sulfate/sludge-based biochar	Calcium sulfate modification	4	280.89	[43]
nHAP/BC	Nano-hydroxyapatite modification	3	383.75-433.69	[44]
BC-Cl	Modification of chloroapatite	4	418.41	This job

The adsorption performance of BC-Cl3 for Pb(II) was compared with that of other reported adsorbents, and the results are shown in Table 4. By comparing the adsorption equilibrium time, we easily found that the equilibrium time of the BC-Cl3-induced Pb(II) adsorption was only slightly longer than that of nHAP /BC, which is consistent with that of calcium sulfate/ sludge-based biochar. By comparing the adsorption capacity of Pb(II), we found that BC-Cl3 has a larger adsorption capacity for Pb(II) than other biochars, except nHAP /BC. The BC-Cl3 in this study has certain advantages in the adsorption of Pb(II) in wastewater, and a higher adsorption capacity can be achieved in a short time. It is an adsorption material with potential application value.

Analysis of Potential Adsorption Mechanisms

Considering that the modified sesame straw composite has a variety of functional groups, the complex adsorption mechanism of Pb(II) on BC-Cl can be illustrated by the schematic diagram in Fig 5.

First of all, heavy metal ions can be fixed by complexing with oxygen-containing functional groups in the material, which is one of the important mechanisms of biochar adsorption of heavy metals. Both FT-IR characterization and composition information indicate that the surface of the composite is rich in oxygen-containing groups, such as carboxylic (–COOH), hydroxyl (–OH), and aromatic (C=C) groups, which can be chemically complexed with metal ions. Previous studies have shown that after the adsorption of Pb(II) by apatite modified biochar, the infrared spectrum shows that the vibration peak of the oxygen-containing functional group shifts and weakens, which indicates that the functional group participates in the adsorption of Pb(II) by apatite modified biochar.

Secondly, Ca^{2+} and other cations on BC-Cl can interact with Pb(II) in aqueous solutions through ion exchange, while PO_4^{3-} or CO_3^{2-} can fix heavy metal ions through co-precipitation reactions, thus forming insoluble precipitation and promoting the removal of heavy metals. The reaction equation is as follows:

$$CaCO_3+Pb(II)\rightarrow PbCO_3\downarrow+Ca^{2+} \quad (8)$$

$$Ca(PO_4)_2+Pb(II)\rightarrow Pb(PO_4)_2\downarrow+Ca^{2+} \quad (9)$$

In addition, the C content of BC-Cl is relatively high, and there are many aromatic carbon components with good electron transfer ability in the composite, which can form cation-π bonds with heavy metal ions. Therefore, apatite modified biochar can interact with heavy metals in various forms and is an excellent potential environmental treatment material for heavy metals.

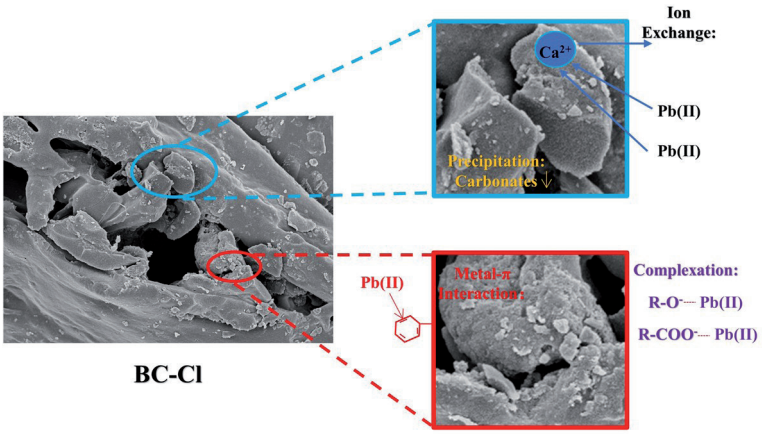

Fig. 5. The schematic diagram of mechanisms for heavy metals adsorbed on the FM-BCs.

Conclusions

In this study, sesame straw, chlorapatite, and hydroxyapatite were used as raw materials to prepare biochar composites modified by apatite co-impregnation, and the adsorption properties of Pb(II) in water by BC-Cl were investigated. The batch adsorption experiments showed that the adsorption capacity of BC-Cl3 was significantly higher than that of BC and HBC. Under the conditions of pH = 5 and a dosage ratio of 600 $mg \cdot L^{-1}$, the removal rate of Pb(II) was the highest (99.87%), and the equilibrium adsorption capacity was 416.16 $mg \cdot g^{-1}$. The adsorption kinetics and thermodynamics of Pb(II) in water by BC-Cl conform to the quasi-second-order model and Langmuir isotherm, respectively, indicating that the adsorption reaction is dominated by chemical adsorption. BC-Cl shows a good prospect of adsorption of Pb(II) in industrial wastewater. The research results provide a basic scientific basis and theoretical reference for the resource utilization of waste biomass and the research and development of environmental functional materials for efficient removal of heavy metals from water.

Acknowledgments

This project has not been supported by any fund. We thank Zihan Chen and Lu Yu for editing the English text of the first draft of the manuscript.

Conflict of Interest

The authors declare no conflict of interest.

References

1. ASKARI S.G., OSKOEI V., ABEDI F., FAR P.M., NAIMABADI A., JAVAN S. Evaluation of heavy metal concentrations in black tea and infusions in Neyshabur city and estimating health risk to consumers. International Journal of Environmental Analytical Chemistry, **102** (19), 7928, **2022**.
2. LI Z., MA Z., VAN DER KUIJP T.J., YUAN Z., HUANG L. A review of soil heavy metal pollution from mines in China: Pollution and health risk assessment. Science of the Total Environment, **468**, 843, **2014**.
3. BOUMAZA B., KECHICHED R., CHEKUSHINA T.V., BENABDESLAM N., SENOUCI K., HAMITOUCHE A., MERZEG F.A., REZGUI W., REBOUH N.Y., HARIZI K. Geochemical distribution and environmental assessment of potentially toxic elements in farmland soils, sediments, and tailings from phosphate industrial area (NE Algeria). Journal of Hazardous Materials, 465, **2024**.
4. ABBA S.I., YASSIN M.A., SHAH S., EGBUERI J.C., ELZAIN H.E., AGBASI J.C., SAINI G., USAMAN J., KHAN N.A., ALJUNDI I.H. Trace element pollution tracking in the complex multi-aquifer groundwater system of Al-Hassa oasis (Saudi Arabia) using spatial, chemometric and index-based techniques. Environmental Research, **249**, 118320, **2024**.
5. NAZ A., CHOWDHURY A., CHANDRA R., MISHRA B.K. Potential human health hazard due to bioavailable heavy metal exposure via consumption of plants with ethnobotanical usage at the largest chromite mine of India. Environ Geochem Health, **42** (12), 4213, **2020**.
6. RAI P.K., LEE S.S., ZHANG M., TSANG Y.F., KIM K.H. Heavy metals in food crops: Health risks, fate, mechanisms, and management. Environment International, **125**, 365, **2019**.
7. NOVIKAU R., LUJANIENE G. Adsorption behaviour of pollutants: Heavy metals, radionuclides, organic pollutants, on clays and their minerals (raw, modified and treated): A review. Journal of Environmental Management, 309, **2022**.
8. LIN M.X., LI F.Y., LI X.T., RONG X.M., OH K. Biochar-clay, biochar-microorganism and biochar-enzyme composites for environmental remediation: a review. Environmental Chemistry Letters, **21** (3), 1837, **2023**.
9. KHEDULKAR A.P., PANDIT B., DANG V.D., DOONG R. Agricultural waste to real worth biochar as a sustainable material for supercapacitor. Science of the Total Environment, 869, **2023**.
10. TAN M. Conversion of agricultural biomass into valuable biochar and their competence on soil fertility enrichment. Environmental Research, 234, **2023**.

11. XIA L., CHEN W., LU B., WANG S., XIAO L., LIU B., YANG H., HUANG C., WANG H., YANG Y., LIN L., ZHU X., CHEN W., YAN X., ZHUANG M., KUNG C., ZHU Y., YANG Y. Climate mitigation potential of sustainable biochar production in China. Renewable & Sustainable Energy Reviews, 175, **2023**.
12. POTNURI R., SURYA D.V., RAO C.S., YADAV A., SRIDEVI V., REMYA N. A review on analysis of biochar produced from microwave-assisted pyrolysis of agricultural waste biomass. Journal of Analytical and Applied Pyrolysis, 173, **2023**.
13. LIANG Z., NEMENYI A., KOVACS G.P., GYURICZA C. Potential use of bamboo resources in energy value-added conversion technology and energy systems. Global Change Biology Bioenergy, **15** (8), 936, **2023**.
14. FENG Z.Q., CAO X., ZHOU B.H., LI H.Q., LIU H.J., YUAN R.F., WANG X., CHEN Z.B., LUO S., CHEN H.L. Influence mechanisms of different stalks on iron species type of magnetic biochar prepared from Fe2O3. Science of the Total Environment, 903, **2023**.
15. ASHRAFI A., RAHBAR-KELISHAMR A., SHAYESTEH H. Highly efficient simultaneous ultrasonic assisted adsorption of Pb (II) by Fe3O4@MnO2 core-shell magnetic nanoparticles: Synthesis and characterization, kinetic, equilibrium, and thermodynamic studies. Journal of Molecular Structure, **1147**, 40, **2017**.
16. GUO X., LI H. Effects of Iron-Modified Biochar and AMF Inoculation on the Growth and Heavy Metal Uptake of Senna occidentalis in Heavy Metal-Contaminated Soil. Polish Journal of Environmental Studies, **28** (4), 2611, **2019**.
17. CHEMERYS V., BALTRENAITE-GEDIENE E., BALTRENAS P., DOBELE G. Influence of H2O2 Modification on the Adsorptive Properties of Birch-Derived Biochar. Polish Journal of Environmental Studies, **29** (1), 579, **2020**.
18. ZHANG J.Q., CHEN Z.J., LIU Y.W., WEI W., NI B.J. Removal of emerging contaminants (ECs) from aqueous solutions by modified biochar: A review. Chemical Engineering Journal, 479, **2024**.
19. XU J., FU M., MA Q., ZHANG X., YOU C., SHI Z., LIN Q., WANG X., FENG W. Modification of biochar by phosphoric acid via wet pyrolysis and using it for adsorption of methylene blue. Rsc Advances, **13** (22), 15327, **2023**.
20. TENG Y., CHEN K., JIANG H., HU Y., SEYLER B.C., APPIAH A., PENG S. Utilization of phosphoric acid-modified biochar to reduce vanadium leaching potential and bioavailability in soil. Environmental Pollution, **344**, 123360, **2024**.
21. 21. FENG Y., GONG J., ZENG G., NIU Q., ZHANG H., NIU C., DENG J., YAN M. Adsorption of Cd(II) and Zn(II) from aqueous solutions using magnetic hydroxyapatite nanoparticles as adsorbents. Chemical Engineering Journal, **162** (2), 487, **2010**.
22. LONG Y., JIANG J., HU J., HU X., YANG Q., ZHOU S. Removal of Pb(II) from aqueous solution by hydroxyapatite/ carbon composite: Preparation and adsorption behavior. Colloids and Surfaces a: Physicochemical and Engineering Aspects, **577**, 471, **2019**.
23. WANG Y., LIU Y., LU H., YANG R., YANG S. Competitive adsorption of Pb(II), Cu(II), and Zn(II) ions onto hydroxyapatite-biochar nanocomposite in aqueous solutions. Journal of Solid State Chemistry, **261**, 53, **2018**.
24. LONG Y., JIANG J., HU J., HU X., YANG Q., ZHOU S. Removal of Pb(II) from aqueous solution by hydroxyapatite/ carbon composite: Preparation and adsorption behavior. Colloids and Surfaces a-Physicochemical and Engineering Aspects, **577**, 471, **2019.**
25. LONG Y., JIANG J., HU J., HU X., YANG Q., ZHOU S. Removal of Pb(II) from aqueous solution by hydroxyapatite /carbon composite: Preparation and adsorption behavior. Colloids and Surfaces a-Physicochemical and Engineering Aspects, **577**, 471, **2019**.
26. MOUHAMADOU S., DALHATOU S., OBADA D.O., FRYDA L., MAHIEU A., BONNET P., CAPERAA C., KANE A., MASSAI H., ZEGHIOUD H. Synthesis of piliostigma reticulatum decorated TiO_2 based composite and its application towards Cr(VI) adsorption and bromophenol blue degradation: Nonlinear kinetics, equilibrium modelling and optimisation photocatalytic parameters. Journal of Environmental Chemical Engineering, **11** (1), **2023**.
27. HAI N.T., LIMA E.C., JUANG R., BOLLINGER J., CHAO H. Thermodynamic parameters of liquid-phase adsorption process calculated from different equilibrium constants related to adsorption isotherms: A comparison study. Journal of Environmental Chemical Engineering, **9** (6), **2021**.
28. KOZLOWSKI C. X-ray photoelectron-spectroscopic studies of carbon-fibre surfaces. Part 5. & mdash; The effect of pH on surface oxidation. Journal of the Chemical Society, Faraday Transactions 1: Physical Chemistry in Condensed Phases, **81** (11), **1985**.
29. CHEN Y., LI M., LI Y., LIU Y., CHEN Y., LI H., LI L., XU F., JIANG H., CHEN L. Hydroxyapatite modified sludge-based biochar for the adsorption of Cu^{2+} and Cd^{2+}: Adsorption behavior and mechanisms. Bioresource Technology, 321, **2021**.
30. BĄK J., GUSTAW S., KOŁODYŃSKA D. The use of eggshells, boiler stone, chalk and marl for the synthesis of novel hydroxyapatite modified biochars for the vanadium removal. Chemical Engineering Journal, 470, **2023**.
31. ADEWUYI A., PEREIRA F.V. Nitrilotriacetic acid functionalized Adansonia digitata biosorbent: Preparation, characterization and sorption of Pb(II) and Cu(II) pollutants from aqueous solution. Journal of Advanced Research, **7** (6), 947, **2016**.
32. DECHAPANYA W., KHAMWICHIT A. Biosorption of aqueous Pb(II) by H3PO4-activated biochar prepared from palm kernel shells (PKS). Heliyon, **9** (7), **2023**.
33. DENG Y.Y., HUANG S., DONG C.Q., MENG Z.W., WANG X.G. Competitive adsorption behaviour and mechanisms of cadmium, nickel and ammonium from aqueous solution by fresh and ageing rice straw biochars. Bioresource Technology, 303, **2020**.
34. DEBNATH S., DAS R. Strong adsorption of CV dye by Ni ferrite nanoparticles for waste water purification: Fits well the pseudo second order kinetic and Freundlich isotherm model. Ceramics International, **49** (10), 16199, **2023**.
35. CORTES J.C., NAVARRO-QUILES A., SANTONJA F.J., SFERLE S.M. Statistical analysis of randomized pseudo-first/second order kinetic models. Application to study the adsorption on cadmium ions onto tree fern. Chemometrics and Intelligent Laboratory Systems, 240, **2023**.
36. WANG D., LUO W., ZHU J., WANG T., GONG Z., FAN M. Potential of removing Pb, Cd, and Cu from aqueous solutions using a novel modified ginkgo leaves biochar by simply one-step pyrolysis. Biomass Conversion and Biorefinery, **13** (9), 8277, **2023**.
37. LIU J., GE Y., WANG G., LIU Y., XU X. Highly efficient removal of U(VI) in aqueous solutions by tea

waste-derived biochar-supported iron-manganese oxide composite. Journal of Radioanalytical and Nuclear Chemistry, **330** (3), 871, **2021**.
38. KUMAR R., SHARMA P., SHARMA P.K., ROSE P.K., SINGH R.K., KUMAR N., SAHOO P.K., MAITY J.P., GHOSH A., KUMAR M., BHATTACHARYA P., PANDEY A. Rice husk biochar – A novel engineered bio-based material for transforming groundwater-mediated fluoride cycling in natural environments. Journal of Environmental Management, 343, **2023**.
39. ZHU J., ZHAO J., ZHOU S., WU C., ZHAO D., JIANG L., LIU S. Study on the removal of Pb and Cd ions from water by peanut shell biochar and its adsorption mechanism. Journal of Southwest Forestry University (Natural Science), **42** (05), 78, **2022**.
40. XIAO Y., WU Z., CUI M., SU R., XIE L., HUANG R. Study on co-modification of biochar and bentonite and lead ion adsorption and stabilization. Journal of Inorganic Materials, **36** (10), 1083, **2021**.
41. ZHANG L., WANG Y., WANG W., LI Y., SUN P., HAN J., JIANG Q. Preparation of magnetic hydroxyapatite/biochar composites and their adsorption properties for Pb(II). Journal of Environmental science, **38** (11), 4360, **2018**.
42. ZHANG G., CHENG H., ZHANG H., SU L., HE X., TIAN X., NING R. Adsorption mechanism of Pb(II) by bisporangium bran biochar and its environmental application potential. Journal of Agricultural and Environmental Sciences, **40** (03), 659, **2021**.
43. LIU R., LIU L., HUANG R., LIU X. Study on the adsorption performance of calcium sulfate/sludge-based biochar to lead in water. Industrial Water Treatment, **41** (05), 46, **2021**.
44. ZHANG L., WANG Y., WANG W., LI Y., SUN P., HAN J., JIANG Q. Preparation of biochar supported nano-hydroxyapatite composites and their adsorption properties for lead ions. Progress in Chemical Industry, **37** (09), 3492, **2018**.